Journal of The Electrochemical Society, **151** (12) D121-D126 (2004)
0013-4651/2004/151(12)/D121/6/$7.00 © The Electrochemical Society, Inc.

Interfacial Properties and Gas Bubble Formation during the Electrolytic Preparation of Fluorine

F. Lantelme[z] and H. Groult*

Laboratoire LI2C-Electrochimie, UMR 7612, Université Pierre et Marie Curie, 75252 Paris cedex 05, France

During the electrolysis of fused KF-2HF strongly adherent bubbles of fluorine gas appear at the surface of the carbon anode. It was observed that the current is passing even when the anode was fully covered with a gas film. Impedance measurements performed in KF-2HF coupled with visual observations with a see-through cell show the existence of a conducting layer beneath the gas film. Experiments were performed to study the bubble growth by transient techniques. The results were interpreted in the frame of a model which shows the predominant role of the interfacial properties. A new approach, introducing capillary forces, leads to the concept of a variable curvature radius at the gas-liquid interface which is in agreement with the observed bubble shape. Digital simulation is used to describe the bubble growth and to calculate the values of interfacial parameters.
 [DOI: 10.1149/1.1810452]

Manuscript submitted March 1, 2004; revised manuscript received April 28, 2004. Available electronically October 28, 2004.

Interfacial properties play an important role in electrochemical reactions involving gaseous components.[1] The formation and growth of gas bubbles has been extensively studied for reactions of industrial interest such as water electrolysis[2] and aluminum preparation.[3] Generally, the bubble evolution obeys a classic mechanism of nucleation, growth, coalescence, detachment, and the rise of bubbles. The size and adherence of bubbles depend on the properties of the liquid-gas interface. For many reactions the contact angle is nearly zero, and the weakly adherent bubbles have a spherical shape. The electrode surface is not very modified by the presence of bubbles and most of the research work deals with the bubble influence on the fluid motion in the vicinity of the electrode.[4]

However, this behavior may change according to the nature of the electrode material and the electrolyte composition. For instance, in the electrolytic preparation of aluminum, when the alumina content of the melt decreases, a correlated increase of the contact angle is obtained. For a low amount of alumina a rapid change in the wetting properties occurs and the contact angle jumps to around 180°. This results in a full coverage of the electrode by the gas phase followed by an increase of the overpotential and appearance of sparkling phenomena. This anode effect is clearly due to the discharge of fluoride ions, which gives rise to fluorocarbon compounds at the surface of the carbon electrode. The solid-liquid interfacial energy is very low and the liquid cryolite does not wet any more the anode.

These phenomena present some similarity with those occurring in the fluorine production which takes place by electrolysis of molten KF-2HF electrolysis at about 100°C. The fluorine gas is formed on carbon anodes and hydrogen evolves on iron cathodes. The body of the cell and the diaphragm are made of Monel.[5,6] The overall process corresponds to the decomposition of hydrofluoric acid, $2HF \rightarrow H_2 + F_2$. Although the thermodynamic potential of HF decomposition was demonstrated to be 2.9 V,[7] a voltage of around 10 V must be applied. The mechanism of fluorine evolution has been extensively studied in the literature.[8,9] In cooperation with the Comurhex Company, the fundamental behavior of fluorine evolution on a carbon anode has been examined.[7,10] In contrast to the aluminum production, no anode effect appears during the electrolysis. However, the anode overpotential is very high, around 2.5 V. This large overpotential is due to the formation of a thin barrier of conducting fluorocarbon (denoted C-F henceforth) at the electrode surface.[11,12] As for the aluminum cells during the anode effect, the fluorine gas bubbles spread over the electrode surface, but this coverage does not hinder the current flow. Recent experiments have shown that, on a horizontal electrode fully covered with a thick fluorine layer, the current is still passing.[13] Owing to this set of experiments, a new representation of the electrode/electrolyte interface was proposed in which a conducting layer is intercalated between the C-F solid layer and fluorine bubbles. The aim of the present paper is to describe some experiments carried out to illustrate this surprising behavior and to develop a model to obtain a better understanding of the reaction mechanism.

Experimental

Experiments were done under fluorine evolution by electrolysis of dehydrated molten KF-2HF at 95°C (water concentration less than 20 ppm). A graphite auxiliary electrode and a Cu/CuF_2 reference electrode (+0.4 V *vs.* Pt-H_2) were used. All potential values are referred to this reference henceforth. The electrochemical cell was equipped with a Plexiglas window, which made visible inspection possible.

A horizontal working electrode facing the top of the cell was used. It was made of a disk of industrial nongraphitized carbon for fluorine production. The disk thickness was 0.5 cm, the diameter varied from 1.6 to 0.4 cm. The lateral part and the bottom of the disk were coated with Teflon. To perform the experiments with a steady fluorinated layer with constant thickness and stoichiometry, the samples were activated at 40 V for 1 min prior to the experiment. The chronopotentiograms and chronoamperograms were obtained with an EG&G PAR model 273 generator.

Results and Discussion

The first set of experiments concerned the electrode behavior at a constant current. The results depended on the electrode diameter and potential. However, all the experiments exhibited similar features. A periodic evolution of gas bubbles occurred, the period depending on the applied current. An abrupt decrease in the potential was shown when the bubble detached from the surface. After a rapid increase of the potential, a plateau was observed before the bubble detachment (Fig. 1).

In a potentiostatic condition, a similar behavior was obtained with periodic evolution of gas bubbles. The current was correlated to the bubble evolution; just after the bubble detachment, the current jumped to a maximum value. Then it decreased quite rapidly and after a few seconds, the decrease became less rapid; just before the bubble detachment a current plateau was obtained. As an example two chonoamperograms are shown in Fig. 2.

To illustrate the process of bubble growing the shape of the gas bubble was recorded during the electrolysis. In Fig. 3, a chronopotentiogram is reported with pictures of the electrode surface at various stages of the experiment. The main characteristics of the experimental results are reported in Table I.

In contrast to the previous results, if the electrode was turned down, the active surface facing the bottom of the cell, the F_2 bubble

* Electrochemical Society Active Member.
[z] E-mail: frl@ccr.jussieu.fr

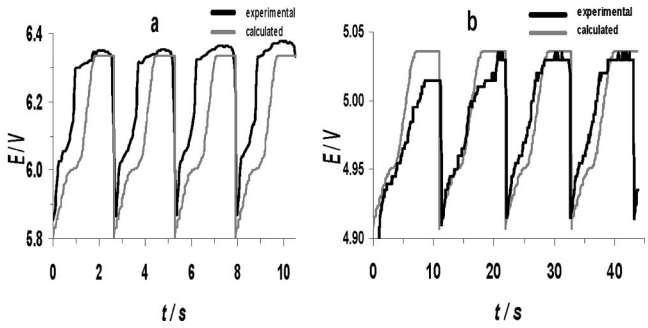

Figure 1. Experimental and calculated chronopotentiograms on a carbon electrode (∅ = 1.2 cm) in KF-2HF at 95°C. (a) I = 400 mA, (b) I = 100 mA.

swell, and tended to spread over the Teflon coating. In this case, the fluorine film became static and the current stopped.[14]

Conducting layer.—Most of the literature studies of gas evolution at an electrode surface, such as H_2, Cl_2, O_2, etc., deal with gas having a weak affinity for the electrode material. This results in the formation of spherical bubbles, which do not adhere to the surface. The gas-liquid layer formed in the vicinity of the electrode induces an important convection of the electrolyte. The situation is very different for the fluorine evolution on a carbon electrode. At the very beginning of the electrolysis process, a layer of fluorocarbon is formed.[15] It is reported in the literature that the formation depends on the surface texture of the carbon.[16] The carbon-fluorine reaction is enhanced in the vicinity of surface pores, and polishing the electrode increases the wettability of the electrode by the electrolyte. In the present experiments, the electrodes are made of carbon used for industrial cells. Surface analysis[14] shows the presence of numerous pores which facilitate the formation of the carbon-fluorine layer which strongly decreases the wettability by the electrolyte.[11] The liquid electrolyte does not wet the anode surface, and a gaseous film rapidly covers the electrode surface.

This gas coverage does not hinder the current flow, and the gas phase continues to grow. To explain this behavior, it has recently been shown that an intermediate conducting layer exists between the C-F layer and the gas bubble. The current is passing through this layer coming from the periphery of the bubble where the gas layer is very thin.[13,14] This hypothesis is supported by the fact that, for a given potential, E, the current is proportional to the perimeter of the disk electrode, not to the electrode area as would be expected (Table I). The existence of the conductive layer is in good agreement with recent electrochemical investigations by impedance spectroscopy which show the existence, at high frequencies, of an additional resistance in series at the electrolyte interface; the characteristic frequency is 200 kHz and the resistivity a few ohms per centimeter,[13] the exact nature of the layer is not yet well known. However, since the layer participates to the fluorine formation it certainly contains a

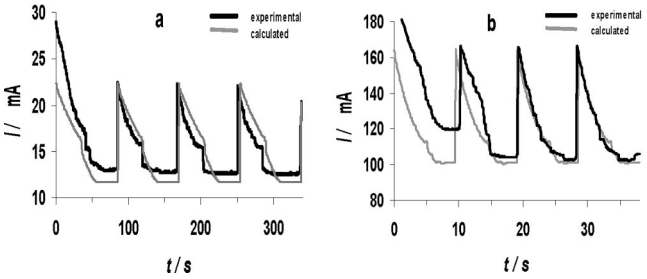

Figure 2. Experimental and calculated chronoamperograms on a carbon electrode (∅ = 1.2 cm) in KF-2HF at 95°C. (a) E = 4.4 V, (b) E = 5.0 V *vs.* Cu/CuF_2.

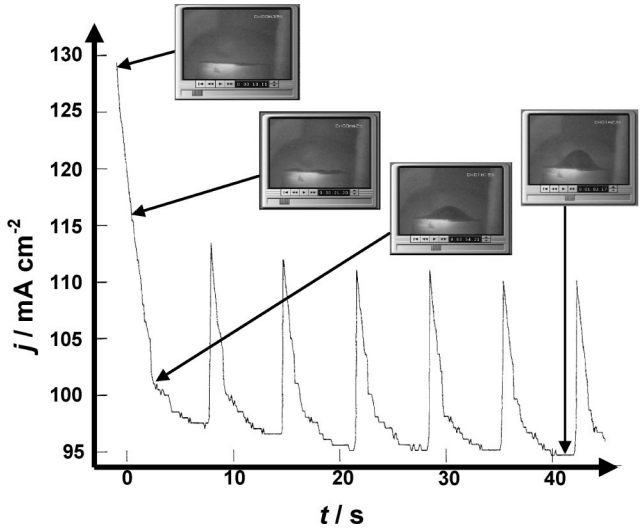

Figure 3. Experimental and calculated chronoamperograms on a carbon electrode (∅ = 1.2 cm) in KF-2HF at 95°C. E = 4.4 V *vs.* Cu/CuF_2. Pictures of the gas bubble at various stages of the electrolysis.

large portion of the liquid electrolyte probably mixed with nascent fluorine and acts as a intermediate between the fluorocarbon barrier at the electrode surface and the fluorine gas bubble.

It should be pointed out that the presence of such an ionic conducting layer presents some similitude with the explanation of Brandon and Kelsall[17] in the case of the bubble departure radii of H_2, Cl_2, O_2 evolution using microelectrodes. They have proposed that a thin liquid film of electrolyte separates the gas and solid phases. Jennings *et al.*[18] have mentioned the existence of a mixed phase at the electrolyte/electrode interface composed of electrolyte and gas. Nevertheless, compared to fluorine bubbles, the shape of these gas bubbles is completely different and their detachment easier.

To fully examine the consequences of this hypothesis a model is presented to take into account the various factors involved in the gas bubble evolution. In recent papers,[14,19] we have studied the contribution of the current coming from the electrochemical reaction in the conducting layer. Now we propose to examine the influence of bubble growth on the electrical current. The principle of this calculation is the following: at the beginning of the calculation, it is considered that a small bubble is present at the electrode surface. During that stage, the lateral part of the bubble remains far from the lateral part of the carbon disk covered with Teflon. The total current results from (*i*) the current I_{free} coming from the electrolysis on the

Table I. Fluorine evolution in KF-2HF at 95°C under a fixed potential on a horizontal anode facing upward, examples of the $I = f(E)$ curves are reported in Fig. 1. r_D, diameter of the disk electrode. E, potential; v, frequency of bubble detachment; I, mean current; j, mean current density; ι, ratio: current/electrode perimeter.

E (V)	r_D (cm)	v (s)	I (mA)	j (mA cm^{-2})	ι (A cm^{-1})
5.5	1.2	4	219	194	57
5.5	1.6	3	269	134	54
5.2	1.2	6	155	137	41
5.2	1.6	4	209	104	42
5.0	1.2	9	104	92	27
5.0	1.6	7	138	69	27
4.7	1.2	24	37	33	10
4.7	1.6	21	66	33	13
4.5	0.8	204	17	34	6
4.5	1.2	83	24	21	6
4.5	1.6	45	20	10	4

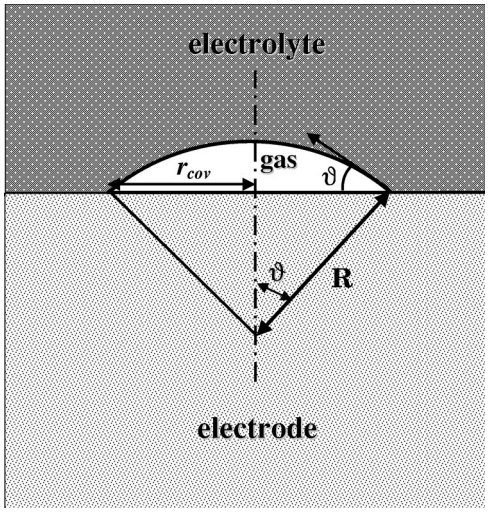

Figure 4. Scheme for the growth of a gas bubble with a constant curvature radius.

electrode surface not covered with the gas, (*ii*) the current I_{cov} coming from the electrode surface covered with the gas bubble. Then, the bubble grows and reaches the lateral part of the carbon disk, I_{free} becomes zero, the total current comes from the reaction in the liquid conducting layer beneath the gas bubble.

Bubble shape and gas evolution.—To interpret the results, a connection is established between the amount of generated gas and the volume of the bubble. The visual examination of the electrode (horizontal and facing upward) during the electrolysis shows that a few small gas bubbles remain at the electrode surface just after the detachment of a fluorine bubble. These bubbles very rapidly coalesce and a unique bubble grows and covers the electrode surface. Then, the bubble swells. A bulge appears in its center and gives rise to a spherical bubble, which detaches and evolves through the electrolyte. A quantitative analysis is carried out considering that the current coming from the uncovered part of the electrode is deduced from the current density and the current coming from the conducting layer beneath the bubble is calculated as described in the previous section. The areas of the covered and uncovered surfaces depend on the gas volume and on the shape of the bubble. The amount of gas is readily calculated from the electrolysis current.

Constant interfacial pressure.—It has been assumed[19] that the curvature radius, R, at the gas-liquid interface is constant and, as a consequence, the bubble has the shape of a spherical cap. According to the classic law,[20] the increment, p_{int}, of pressure due to the interface curvature, R, obeys the equation

$$p_{int} = p_{bub} - p_{ext} = 2\frac{\gamma_{GL}}{R} \qquad [1]$$

p_{bub}, is the pressure inside the bubble, p_{ext} is the external pressure, and γ_{GL} is the gas-liquid surface tension. The volume, V, of the bubble is deduced from the number of moles of gas, n_{F2}, generated by the electrolysis

$$V = \frac{n_{F2}RT}{p_{bub}} \qquad [2]$$

From the formula of the volume of the spherical cap with a contact angle, ϑ, (Fig. 4). It is found

$$R^3 = \frac{3V}{\pi[2 - \cos\vartheta(\sin^2\vartheta + 2)]} \qquad [3]$$

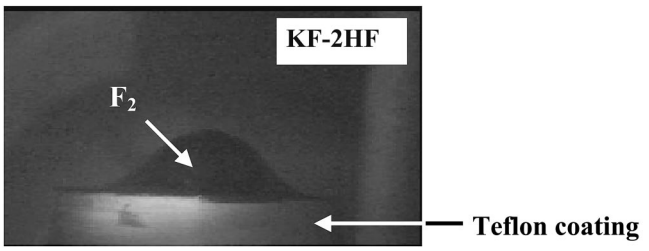

Figure 5. *In situ* image of a bubble at a carbon electrode facing the top of electrochemical cell, $E = 4.5$ V *vs.* Cu/CuF_2, in KF-2HF at 95°C. The bubble contains around 2 μmoles of fluorine; the volume is estimated to be 60 mm^3.

According to Fig. 5, the radius of the disk covered with the bubble is

$$r_{cov} = R \sin\vartheta \qquad [4]$$

The area of the covered surface is

$$S_{cov} = \pi R^2 \sin^2\vartheta \qquad [5]$$

For an electrode of radius r_D, the area of the bubble-free electrode surface is

$$S_{free} = \pi r_D^2 - S_{cov} \qquad [6]$$

For an electrode maintained at a fixed overpotential, η_T, the total current, I_{tot}, comes from the contribution of the two areas. The free area contribution is

$$I_{free} = S_{free} j_0 \exp\left(\frac{\alpha nF}{RT}\eta_T\right) \qquad [7]$$

According to the literature,[21] the transfer coefficient, α, is close to 0.3. The current, I_{cov}, coming from the covered surface, is deduced from the calculation described in previous papers[14,19] for a conducting disk of radius r_{cov}, then, $I_{tot} = I_{cov} + I_{free}$. To examine the bubble growth, a finite step difference technique is used again. The time of the experiment (between the two detachments of gas bubbles) is divided into small time intervals, Δt. During that time, the number of moles of fluorine generated by the electrochemical reaction is

$$\Delta n_{F2} = \frac{I_{tot}\Delta t}{2F} \qquad [8]$$

F is the Faraday constant. The total number of moles in the gas phase at the time t is

$$n_{F2}(t) = n_{F2}(t - \Delta t) + \Delta n_{F2} \qquad [9]$$

This procedure has been used in a previous paper[19] to describe the electrode behavior with a fluorine evolution. However, the model should now be improved. Indeed, the *in situ* observation shows that the shape of the bubble is not exactly that of a spherical cap. The periphery of the bubble is flattened, and the adherent bubble has the shape of a flying saucer (Fig. 5). Such a shape is attributed to the presence of capillary forces, which are introduced in the analysis developed in the following section.

Variable interfacial pressure.—In order to obtain a more realistic bubble shape, it is assumed that a capillary force exists between the electrode surface and the gas-liquid interface. As a simplified assumption a phenomenological approach is used; the capillary pressure at the gas-liquid interface is supposed to be proportional to the reverse of the distance, h_{cap} (Fig. 6)

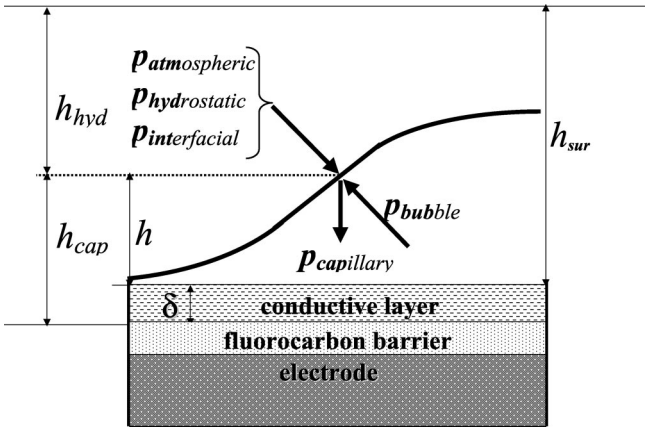

Figure 6. Scheme for the pressure balance at the gas-liquid interface.

$$p_{cap} = \frac{K}{h_{cap}} \quad [10]$$

with $h_{cap} = h + \delta$. The thickness, δ, of the conducting layer has been estimated from *in situ* observations[22] coupled with the exploitation of impedance diagrams,[13] $\delta = 0.3$ mm. K is the proportionality constant which is analogous to the surface tension. In order to obtain an accurate description of the phenomena the hydrostatic pressure, p_{hyd}, is introduced in the model

$$p_{hyd} = h_{hyd} dg \quad [11]$$

d is the density of the electrolyte and g the gravitational acceleration. h_{hyd}, the distance to the electrolyte surface, is determined from the distance, h_{sur}, between the surface of the conductive layer and electrolyte surface, $h_{hyd} = h_{sur} - h$. The external pressure, introduced in the previous section (Eq. 1), is

$$p_{ext} = p_{atm} + p_{hyd} \quad [12]$$

p_{atm} is the atmospheric pressure. The pressure inside the bubble obeys the equation

$$p_{bub} = p_{atm} + p_{hyd} + p_{cap} + p_{int} \quad [13]$$

In the present situation, R varies all along the gas-liquid interface. At a distance close to the electrode, the term p_{cap} is large and the value of p_{int} can be negative which corresponds to a concave curve. In this case, according to Eq. 1, R is negative. At a time, t, the volume of the bubble again obeys Eq. 2. However, the gas bubble no longer has the shape of a spherical cap and Eq. 3 does not apply. To solve the problem a step by step process is used. The interface

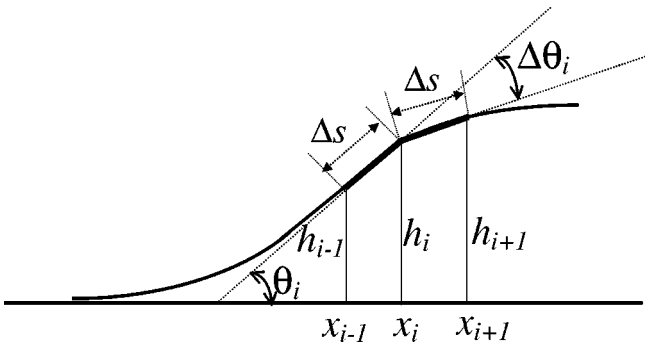

Figure 7. Sequence for the calculation of the gas-liquid profile.

profile is divided into small distance intervals, Δs, as described in Fig. 7, the coordinates of a point $i + l$ is deduced from the coordinates, x_i and h_i of the point i. According to the definition of the curvature radius, the angular increment, $\Delta\theta_i$, between the tangents at the points i and $i + l$ is

$$\Delta\theta_i = -\frac{\Delta s}{R_i} \quad [14]$$

By convention $\Delta\theta_i$, is positive for a concave curve. The angle of the line i, $i + l$ with the electrode surface is

$$\theta_{i+l} = \theta_i + \Delta\theta_i \quad [15]$$

θ_i is the angle of the line $i - l$, i *vs.* the x axis. The coordinates of the point $i + l$ are

$$x_{i+l} = x_i + \Delta s \cos \theta_{i+l} \quad [16]$$

$$h_{i+l} = h_i + \Delta s \sin \theta_{i+l} \quad [17]$$

R_i is determined from a trial and error process. An approximate value of p_{bub} is arbitrarily chosen and R_i is deduced from the interface pressure (Eq. 1) given by

$$p_{int}(i) = p_{bub} - p_{hyd}(i) - p_{cap}(i) - p_{atm} \quad [18]$$

$p_{hyd}(i)$ and $p_{cap}(i)$ obey Eq. 10 and 11. The origin of the x axis is chosen at the border of the bubble, at the triple-contact, gas-solid-liquid. At that point the contact angle is nearly zero. The capillary pressure, p_{cap}, can be large; it results (Eq. 18) show that the interfacial pressure is negative, and the curve is concave. In this region, the angle, θ_i, is increasing. However, as the distance h increases, the angle increment $\Delta\theta_i$ decreases and becomes null. That situation corresponds to the inflexion point of the interface profile. Then, $\Delta\theta_i$ is negative and θ_i decreases. The abscissa, x_k, for which $\theta_k = 0$, is the radius, r_{cov}, of the gas bubble. The volume of the bubble is calculated from the summation of the volume of the elementary tubes of height h_i and of thickness, $\Delta s \cos \theta_{i+l}$

$$\Delta V_i = \frac{\pi}{2}(x_i + x_{i+l})(x_{i+l} - x_i)(h_i + h_{i+l}) \quad [19]$$

The calculated volume, V_{cal}, is compared to the volume, V, deduced from the number moles of fluorine coming from the electrolysis (Eq. 2 and 9). The pressure, p_{bub}, is varied, in order that $V_{cal} = V$. If $V_{cal} > V$, p_{bub} is increased, the bubbles profile becomes more flat and V_{cal} decreases. As indicated above, a Trial and error process is used which rapidly converges toward the right value.

As an example, the profile for a bubble containing 1.8 μmoles of fluorine is shown in Fig. 8a. The following parameters were used: $p_{atm} = 1$ atm, $h_{sur} = 1$ cm, $d = 1.98$ g cm^{-3}, $g = 981$ cm s^{-2}, $\gamma_{GL} = 750$ dyne cm^{-1}, $K = 740$ dyne cm^{-1}, $p_{bub} = 1.0086$ atm.

To study the bubble growth during the electrolysis a step-by-step procedure is used. The time is divided into small time intervals, Δt. The current at a time, t, is deduced from the current coming from the covered and uncovered areas of the electrodes as described in section Constant interfacial pressure. However, when the radius of the covered area, r_{cov}, tends to the electrode radius, r_D, the current is still passing in the very thin layer at the periphery of the bubble. The additional resistance, R_{add}, depends on the thickness of the layer and is assumed to be proportional to tan θ_l. The angle θ_l is the value of θ_i in the external ring, θ_l is equal to the contact angle, ϑ. In the present model the following empirical equation is used

$$R_{add} = \frac{\lambda\rho}{2\pi r} \tan \theta_l \quad [20]$$

Table II. Values of the parameters introduced in the model for the calculated curves.

Experiments		γ_{GL} (dyne cm^{-1})	j_0 (A cm^{-2})	K (dyne cm^{-1})	ρ (Ω cm)	λ
Constant *E*	5.0 V	1000	1.1×10^{-10}	1000	0.5	40
	4.4 V	1250	3.2×10^{-9}	1250	0.25	100
Constant *I*	100 mA	350	3.8×10^{-10}	350	2	40
	400 mA	350	1.6×10^{-11}	350	2	48
Mean values		750	9.2×10^{-10}	740	1.2	57

λ is a proportionality constant. Since the electrode surface is fully covered, fluorine gas generated by the clectrolysis induces a swelling of the bubble. The pressure inside the bubble is increased and the contact angle is growing in order that the calculated volume of the bubble fits the experimental volume deduced from the amount of gas. The bubble growth leads to the formation of a spherical excrescence, which soon detaches from the electrode surface under the action of the hydrostatic pressure. During that last phase, due to the growth of the evolving bubble, the pressure remains nearly constant. It results in a current plateau just before the detachment of the bubble.

The various parameters introduced in the model are adjusted in order to obtain simulated curves which fit the experimental curves. There are five parameters to be adjusted. The parameters do not have the same influence all along the transient response. After the bubble detachment, the surface covered with the gas is quite small and the electrochemical response is mainly driven by the charge-transfer process, *i.e.*, by the value the exchange current density, j_0. In the same way, just before the bubble detachment, the overpotential at the border of the bubble plays an important role which depends on the value of the parameter λ. Moreover, as a simplifying assumption, it is assumed that the values of the surface tensions, γ_{GL} and K, are equal. Indeed, preliminary calculations show that independent changes of γ_{GL} and K do not improve the quality of the fitting process.

Thus, taking into account the above remarks, we proceed as follow. The curve (between two bubble detachments) is divided into three parts. In a preliminary stage, the first part of the curve is used to calculate j_0 by a least square method, a mean values of the other parameters is used. Then, the first and second parts of the curve are used to calculate $\gamma_{GL} - K$ and ρ by a least square method. Finally, the whole curve is used to calculate λ. The definitive stage is carried out by repeating the three above least square calculations, but now the values of the parameters required by the calculation are those found in the preliminary stage.

The values of the parameters used in the calculation are reported in Table II. A quite large scatter of the values is obtained from one experiment to another, which certainly reflects the heterogeneous nature of industrial carbon anodes. However, the calculated chronoamperograms and chronopotentiograms (Fig. 1, 2) show that the model can be considered as a good representation of the complex process of gas-evolving electrolysis with strongly adherent bubbles. The shape of the fluorine bubble at various stages of the electrolysis is shown in Fig. 8. In contrast to the flat bubble obtained at the beginning of the growth (Fig. 8a), the bubble height just before the detachment (Fig. 8d), is now greater than the radius of the contact disk (bubble electrode).

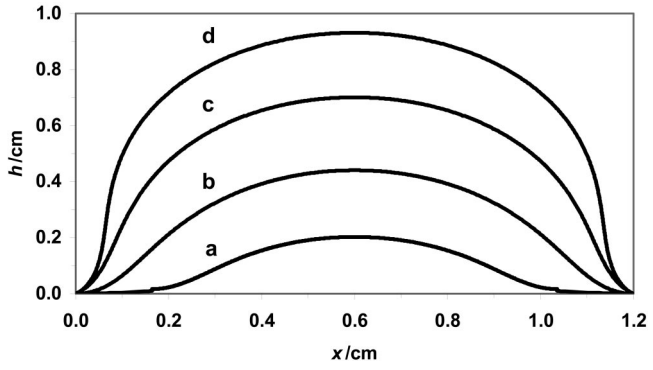

Figure 8. Calculated profile for bubbles of various volumes. (a) 55, (b) 220, (c) 460, (d) 700 mm^3.

Conclusions

The present simplified model is an attempt for a better understanding of the mechanism of fluorine evolution at the surface of a carbon electrode. It takes into account the characteristic features of the process: (*i*) the strong adherence of fluorine gas at the electrode surface, (*ii*) the existence of an electrolytic current even when the electrode is fully covered with the gas film, (*iii*) the flat bubble with a nearly null contact angle. The experimental observations lead to postulate the existence of a thin conducting layer beneath the gas bubble. The variable curvature radius of the bubble is the consequence of a skin effect due to the influence of capillary forces. Digital simulation is used to calculate the electrode reaction from the electrochemical and interfacial properties. The model provides a basis for a quantitative study of the anode behavior in fluorine cells.

Acknowledgments

Grateful acknowledgements are made to the Comurhex-Areva Company for its joint support of the research project and to Dr. J.-P. Caire (ENSEEG-INPG, Saint Martin d'Hères Cedex, France) for helpful discussions.

Université Pierre et Marie Curie assisted in meeting the publication costs of this article.

List of Symbols

d	density of the electrolyte
E	electrode potential
E^0	equilibrium potential of the fluorine evolution
F	Faraday constant
g	gravitational acceleration
h	distance of the gas-liquid interface from the conducting layer
h_{cap}	distance of the gas-liquid interface from the electrode surface
h_{hyd}	distance of the gas-liquid interface from the electrolyte surface
h_{sur}	distance of the conducting layer from the electrolyte surface
I	current intensity
I_{cov}	current coming from the conducting layer covered with the fluorine bubble
I_{free}	current coming from electrode area not covered with the fluorine bubble
I_r	current flowing through the ring of radius r
I_{tot}	total current flowing through a carbon disk electrode
j	current density
j_0	exchange current density
K	constant for the calculation of the capillary pressure (Eq. 10)
n	number of electrons
n_{F2}	number of moles of fluorine in the bubble
p_{atm}	atmospheric pressure
p_{bub}	pressure inside the bubble
p_{hyd}	hydrostatic pressure
p_{int}	interfacial pressure
r	radius of an elementary ring in the disk covered with the gas bubble
r_D	radius of the carbon disk electrode
r_{cov}	radius of the carbon disk electrode covered with the gas bubble
R	gas constant
R	curvature radius
R_i	curvature radius at the point i of the gas liquid interface

R_{add} additional resistance at the periphery of the bubble
S_{cov} area covered with the gas bubble
S_{free} area of the bubble-free electrode
t time
T absolute temperature
V bubble volume deduced from n_{F2}
V_{cal} bubble volume deduced from the bubble shape

Greek

α anodic transfer coefficient
γ_{GL} gas-liquid surface tension
δ thickness of the condensed layer
Δr radius increment
Δs distance increment of the interface profile
Δt time increment
λ constant used to calculate R_{add}
η_T total anodic overpotential
θ_i angle of the tangency at the point i of the gas liquid interface with the electrode plane
ϑ contact angle
ρ resistivity of the conducting layer

References

1. S. Lubetkin, *Electrochim. Acta*, **48**, 357 (2002).
2. H. Vogt, *Electrochim. Acta*, **42**, 2695 (1997).
3. F. Lantelme, D. Diamanacos, and J. Chevalet, *Electrochim. Acta*, **23**, 717 (1978).
4. G. Kreysa and M. Kuhn, *J. Appl. Electrochem.*, **15**, 517 (1985).
5. M. Jaccaud, R. Faron, D. Devilliers, and R. Romano, *Ulmann's Encyclopedia of Industrial Chemistry*, Vol. A11, p. 293, VCH, Weinheim (1988).
6. J. F. Ellis and G. F. May, *J. Fluorine Chem.*, **33**, 133 (1986).
7. D. Devilliers, F. Lantelme, and M. Chemla, *J. Chem. Phys.*, **76**, 28 (1979).
8. A. J. Rudge, in *Industrial Chemical Processes*, A. T. Kuhn, Editor, Chap. 1, Elsevier, Amsterdam (1971).
9. L. Bai and B. E. Conway, *J. Appl. Electrochem.*, **18**, 839 (1988).
10. H. Groult, *J. Fluorine Chem.*, **119**, 173 (2003).
11. H. Groult, S. Durand-Vidal, D. Devilliers, and F. Lantelme, *J. Fluorine Chem.*, **107**, 247 (2001).
12. N. Watanabe, T. Nakajima, and H. Touhara, *Graphite Fluorides*, Vol. 8, Elsevier, Amsterdam (1988).
13. H. Groult and F. Lantelme, *J. Electrochem. Soc.*, **148**, E13 (2001).
14. H. Groult, D. Devilliers, F. Lantelme, J.-P. Caire, M. Combel, and F. Nicolas, *J. Electrochem. Soc.*, **149**, E485 (2002).
15. D. Devilliers, F. Lantelme, and M. Chemla, *J. Fluorine Chem.*, **35**, 220 (1987).
16. D. Devilliers, B. Teisseyre, M. Vogler, and M. Chemla, *J. Appl. Electrochem.*, **20**, 91 (1990).
17. N. P. Brandon and G. H. Kelsall, *J. Appl. Electrochem.*, **5**, 475 (1984).
18. D. Jennings, A. T. Kuhn, J. Stepanek, and R. Whitehead, *Electrochim. Acta*, **20**, 903 (1975).
19. F. Lantelme, H. Groult, and F. Nicolas, in *Proceedings of International Symposium on Ionic Liquids*, p. 399, Department Material Technology, Norwegian University, Trondheim, Norway (2003).
20. J. T. Davies and E. K. Rideal, *Interfacial Phenomena*, Academic Press, San Diego, CA (1961).
21. F. Nicolas, H. Groult, D. Devilliers, and M. Chemla, *Electrochim. Acta*, **41**, 911 (1996).
22. H. Roustan, Ph.D. Thesis, ENSEEG-INPG, Saint Martin d'Hères, Grenoble, France (1998).